

Free-electron maser oscillator experiment in the UHF regime

R. Drori, E. Jerby *, A. Shahadi

High-Power Microwave Laboratory, Faculty of Engineering, Tel Aviv University, Ramat Aviv 69978, Israel

Abstract

A nonrelativistic electron beam (< 4 keV) travels in this experiment in a non-dispersive waveguide along a planar undulator and an axial magnetic fields. The electron beam has a Gaussian pulse shape with a 1 ms pulse width. Two distinct radiation bursts are observed during the electron energy sweep. Each burst contains a different range of microwave frequencies. One burst corresponds to the FEM interaction, at ~ 0.8 GHz. The other burst corresponds to the cyclotron resonance interaction, at ~ 5 GHz. This experiment demonstrates an FEM operation in an extremely long wavelength (37.5 cm) in the UHF regime.

1. Introduction

A free-electron maser (FEM) experiment in the UHF regime (< 1 GHz) is presented. This FEM operates also in a mode of a cyclotron resonance maser (CRM) at ~ 5 GHz.

The static magnetic field is produced in this experiment by a combination of a solenoid and a planar undulator [1] as shown in Fig. 1. The total magnetic field on-axis is given by $B_0 \cong \hat{x}B_w \cos k_w z + \hat{z}B_0$, where B_0 and B_w are the axial magnetic field and the wiggler amplitudes, respectively, and k_w is the wiggler periodicity. The electron trajectory is, consequently, a superposition of a wiggling motion and a cyclotron motion. The cyclotron wavenumber is $k_c = \omega_c / \bar{v}_z$, where \bar{v}_z is the electron average axial velocity component. $\omega_c = eB_0 / \gamma m$ is the angular cyclotron frequency, and e , m , and γ are the electron charge, mass, and relativistic factor, respectively.

The superposition of the cyclotron and the wiggling motions results in two corresponding conditions for synchronism between the electrons and a TEM-wave in the non-dispersive waveguide. The FEM resonance condition is

$$\omega_{\text{FEM}} = \frac{\bar{v}_z k_w}{1 \pm \bar{v}_z / c}, \quad (1a)$$

and the cyclotron resonance condition is

$$\omega_{\text{CRM}} = \frac{\omega_c}{1 \pm \bar{v}_z / c}, \quad (1b)$$

where the \pm signs correspond to forward and backward waves in the oscillator cavity.

During the electron energy sweep in the Gaussian pulse, the undulator and the cyclotron interactions may excite different radiation frequencies according to Eqs. (1a) and (1b). These interactions are expected in different electron energies and longitudinal cavity modes.

2. Experimental setup

A general view of the FEM experimental device with the non-dispersive waveguide is shown in Fig. 1. The experimental setup is based on the CRM experiment [2] at Tel Aviv University. The oscillator tube consists of a planar-diode electron gun, a coplanar waveguide, a solenoid, and a planar folded-foil undulator. A low-energy electron beam is injected into the waveguide and interacts with the TEM wave. The electron beam is dumped at the exit of the interaction region onto a collector which is also used to measure the electron current. The experimental parameters are listed in Table 1.

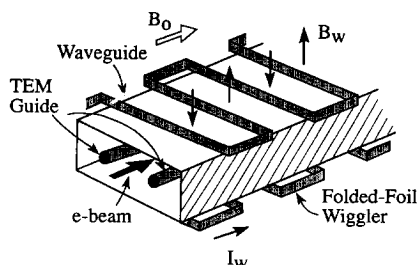


Fig. 1. A scheme of the low-voltage FEM in a non-dispersive waveguide.

* Corresponding author. Tel. +972 3 6408048, fax +972 3 6423508, e-mail jerby@taunivm.tau.ac.il.

Table 1
Experimental parameters

Electron beam		
Energy	< 4	[keV]
Current	< 0.5	[A]
Pulse width	~ 1	[ms]
Magnetic field		
Uniform solenoid	2.0	[kG]
Folded-foil undulator:		
Strength	0.2	[kG]
Period	2.0	cm
TEM waveguide		
Rectangular tube	0.9 × 0.4	[in. ²]
Parallel wires:		
Wire diameter	1.9	[mm]
Distance between centers	11	[mm]
Cavity length	75	[cm]
Microwave output frequency		
Pulse A – Cyclotron	~ 5	[GHz]
Pulse B – FEM	~ 0.8	[GHz]

Three synchronized pulsers generate the solenoid, the e-gun, and the wiggler pulses, as described in Ref. [2]. The e-gun pulser [3] and the high-current wiggler pulser are triggered at the peak of the 20 ms solenoid pulse.

The undulator used in this experiment is a coaxially-fed folded-foil wiggler as described in Ref. [4]. The wiggler strength B_w depends on the current I_w in its windings and is given by $B_w = (2\mu_0 I_w N / \lambda_w) \text{sech}(k_w h / 2)$, where λ_w is the wiggler period, N is the number of winding layers, and h is the wiggler gap. In this experiment, $\lambda_w = 2$ cm, $h = 1.4$ cm, $I_w \leq 400$ A, and $N = 3$. The maximum wiggler magnetic field on-axis is 0.33 kG.

The non-dispersive waveguide shown in Fig. 1 consists of two metal wires stretched along a standard WR90 rectangular tube. The wires are supported by two small ceramic (Macor) holders at the center of the waveguide. The impedance of the coplanar waveguide is $\sim 200 \Omega$. The cavity is terminated at both ends by two partial mirrors. The mirror near the electron gun has a hole at the center for the electron beam entrance. The mirror at the collector has two SMA (50 Ω) RF connectors connected outside the cavity by a wire which forms a small antenna for the output detection as shown in Fig. 2. These terminations form a cavity with a low quality factor ($Q \sim 200$). Cold measurements of the 75 cm cavity show resonance frequencies separated by ~ 200 MHz, with small deviations related to the reactive loads of the partial mirrors at the ends of the waveguide.

The RF power generated in the oscillator is detected by the apparatus shown in Fig. 2. The output signal is sampled by a small dipole antenna and is split into two arms. In one arm, the signal is attenuated and detected by an HP8474 barrier detector. In the other arm, the signal is

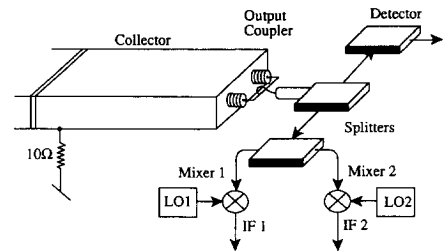


Fig. 2. The microwave diagnostic setup.

split again into two mixers. It is mixed with two local oscillator (LO) signals generated by two external RF oscillators. The mixer outputs are filtered by the internal 20 MHz low-pass filter of a Tektronix TDS 540 digital oscilloscope. This arrangement enables the simultaneous heterodyne measurement of two frequencies in the maser radiation output. In particular, the mixer heterodyne outputs can show the spectral contents of the FEM and the

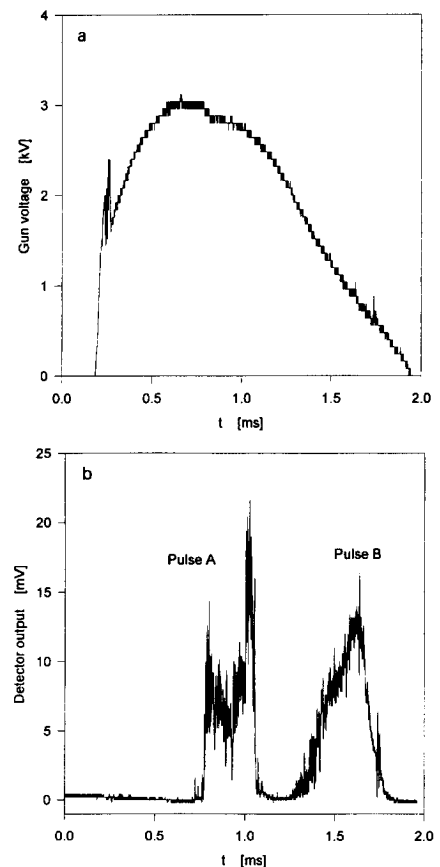


Fig. 3. Typical experimental measurements of two radiation bursts in a single shot. (a) The electron gun voltage. (b) The microwave detected power.

CRM interactions shifted by the corresponding LO frequency.

3. Experimental results

Typical signal measurements of the FEM oscillator are presented in this section. Fig. 3a shows the voltage variation of the electron pulse vs. time. The microwave power excited in the oscillator is shown in Fig. 3b as the power detector output. Two microwave pulses, denoted by A and B, are observed in the detector output in Fig. 3b in the energy levels 2.7 keV and 0.9 keV, respectively. Similar signals have been obtained in over one hundred shots in this experiment. The double heterodyne detection provides a simultaneous measurement of the center frequencies of the two microwave pulses. Each mixer output correlates clearly with each RF pulse. The results show that a 4.93 GHz mixer output coincides with pulse A, and a 0.80 GHz mixer output coincides with pulse B.

A parametric analysis shows an agreement between the

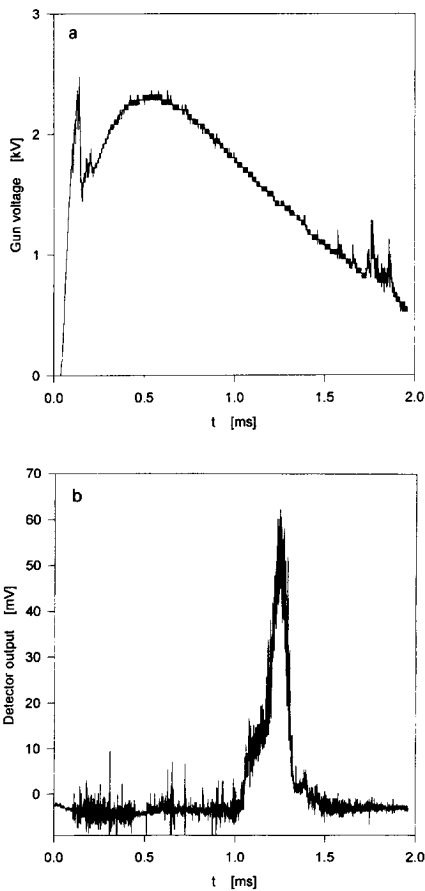


Fig. 4. Typical experimental measurements of one radiation burst in a low-energy electron beam. (a) The electron gun voltage. (b) The microwave detected power.

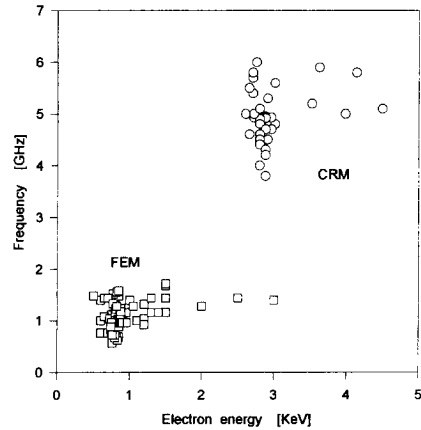


Fig. 5. A frequency–energy map of the FEM and CRM bursts in a 0.4–6.0 GHz LO scan.

tuning relations in Eqs. (1a) and (1b) and the operating conditions of pulses B and A, respectively. Hence, pulse A corresponds to the cyclotron resonance interaction, and pulse B corresponds to the FEM interaction.

A solely FEM interaction is presented in Figs. 4a and 4b, which show the electron gun voltage, and the detector output, respectively. The FEM emission is observed at 825 MHz, without an accompanied CRM interaction. The peak energy in this case, 2.5 keV, is too small to excite the CRM interaction, as observed in the previous example shown in Fig. 3.

A summary of runs performed in this experiment with various LO frequencies in the range of 0.4 GHz to 6 GHz is presented in Fig. 5 in a form of a frequency–energy map. The circles and squares denote observations of mixer outputs in pulse A and pulse B, respectively, with various LO frequencies. Two distinct groups are clearly observed in the map. The spectral content of pulse A is centered around 5 GHz (± 1 GHz) with an electron beam energy centered around 3 keV. The other group in the map, related to pulse B, is centered around 1 GHz and 1 keV. The average values of the two groups (5 GHz at 3 keV for pulse A, and 1 GHz at 1 keV for pulse B) agree well with the corresponding tuning conditions of Eqs. (1b) and (1a). Hence, pulses A and B obtained in many shots are related to the CRM and FEM interactions, respectively. The spectral line widening of the radiation observed might be related to various causes including the axial velocity spread of the electrons, the solenoid field non-uniformity at its ends, and the narrow spikes observed in the detected power.

4. Conclusions

This experiment demonstrates FEM and CRM interactions with TEM modes in a non-dispersive waveguide. The operating FEM frequency is measured in the UHF regime

(< 1 GHz) with an electron energy around 1 keV. In higher energies, around 3 keV, the cyclotron interaction is excited at ~ 5 GHz, in addition to the FEM interaction. For the CRM interaction, the undulator acts as a distributed kicker which rotates the electron beam, as described in Ref. [5].

The FEM operates in this experiment in an exotic operating regime, in which $\lambda \gg \lambda_w$. To the best of our knowledge [6], this is a first demonstration of a low-voltage FEM operation in the UHF regime.

Acknowledgement

This work is supported in part by the Abraham Shechterman Foundation.

References

- [1] Y.Z. Yin and G. Bekefi, J. Appl. Phys. 55 (1984) 33.
- [2] A. Shahadi, E. Jerby, M. Korol, R. Drori, M. Sheinin, V. Dikhtiar, V. Grinberg, I. Ruvinsky, M. Bensal, T. Harel, Y. Baron, A. Fruchtmann, V.L. Granatstein and G. Bekefi, these Proceedings (16th Int. Free Electron Laser Conf., Stanford, CA, USA, 1994) Nucl. Instr. and Meth. A 358 (1995) 143.
- [3] V. Grinberg, E. Jerby and A. Shahadi, *ibid.*, p. 327.
- [4] A. Sneh and E. Jerby, Nucl. Instr. and Meth. A 285 (1989) 294.
- [5] A.C. DiRienzo, G. Bekefi, C. Chen and J.S. Wurtele, Phys. Fluids B 3 (1991) 1755.
- [6] H.P. Freund and V.L. Granatstein, Ref. [2], p. 551.